Acta of Bioengineering and Biomechanics Original paper
Vol. 21, No. 2, 2019 DOI: 10.5277/ABB-01342-2019-02

Numerical reconstruction of injuries in a real world minivan-to-pedestrian collision

GUIBING LI[1], ZHENG TAN[1], XIAOJIANG LV[2, 3], LIHAI REN[4]*

[1] School of Mechanical Engineering, Hunan University of Science and Technology, Xiangtan, China.
[2] State Key Laboratory of Advanced Design and Manufacturing for Vehicle Body, Hunan University, Changsha, China.
[3] Zhejiang Key Laboratory of Automobile Safety Technology, Geely Automobile Research Institute, Ningbo, China.
[4] Key Laboratory of Advanced Manufacturing Technology for Automobile Parts, Ministry of Education, Chongqing University of Technology, Chongqing, China.

Purpose: The purpose of this study was to evaluate the capability of the Total Human Model for Safety (THUMS) – pedestrian model in predicting pedestrian injuries, and to investigate pedestrian injury mechanisms in minivan collisions via numerical reconstruction of a real world minivan-to-pedestrian impact case. *Methods:* A typical minivan-to-pedestrian collision case was selected from the In-depth Investigation of car Accidents in Changsha (IVAC) database. The THUMS middle-size adult male FE model and a minivan front FE model were then employed to represent the case participants and injuries to the pedestrian's lower limb, thorax and head were reconstructed. Finally, the capability of the THUMS model in predicting pedestrian injuries and pedestrian injury mechanisms in minivan collisions were analyzed through comparisons between predictions and the accident data. *Results:* The results show that the THUMS has a good capability in predicting pedestrian thorax injuries, but a lower prediction of leg bending moment and brain strain. The extra bull bar concentrates crash load to pedestrian's leg and raises tibia/fibula fracture risk, thorax injuries in the struck side are mainly from direct contact at the lower chest level, lung injury in the non-struck side could be caused by inertia force from the heart. Rotational acceleration shows good match with brain strain and could be the key mechanism for concussion. *Conclusions:* The results suggest that further improvement in biofidelity of the THUMS model is still needed. The findings also offer basic understanding on pedestrian injury mechanisms in minivan collisions.

Key words: *pedestrian injury, minivan-to-pedestrian collision, accident reconstruction*

1. Introduction

Pedestrians are regarded as an extremely vulnerable and high-risk group of road users since they are unprotected during vehicle impacts. The report of World Health Organization indicates that pedestrians account for about 22% of all deaths on the world's roads, and this proportion is much higher in low income area [28]. Accident data show that injuries to pedestrians' head, thorax and lower limbs dominate all AIS2+ injuries in vehicle-to-pedestrian crashes [20]. A good understanding of injury mechanisms of these body regions in real world impact scenarios is important for pedestrian protection [14], [20]. Accident reconstruction using numerical simulations provides an effective approach for this [2], [8], [17], [23].

Multi-body and finite element (FE) human body models were used as the main tools for predicting pedestrian kinematics and injuries in real world vehicle-to-pedestrian collisions in previous studies. For example, Nie et al. [17] reconstructed real world crashes using multi-body human body models to understand pedestrian kinematics in vehicle impacts. But detailed analysis of injury biomechanics in crashes are not available in this study due to the high simplification of multi-body human body models. Thus FE modeling was widely used for prediction of detailed injury biomechanical in real world vehicle-to-pedestrian collisions. Huang et al. [8] reconstructed pedestrian head

* Corresponding author: Lihai Ren, Key Laboratory of Advanced Manufacturing Technology for Automobile Parts, Ministry of Education, Chongqing University of Technology, 69 Hongguang Ave, Banan Qu, Chongqing Shi 400052, Chongqing, China.
Received: March 14th, 2019
Accepted for publication: April 17th, 2019

injuries using an isolated FE human head model to build the relationships between predicted physical parameters and real pedestrian head injuries in accidents. Isolated FE lower limb models were also used for reconstruction of pedestrian leg injuries, such as the study from Wang et al. [23], where an FE lower limb model was employed to predict long bone fractures in real world passenger car-to-pedestrian collisions. However, these studies on reconstruction of detailed pedestrian injuries in real world crashes only focused on a particular body region, using isolated models of the corresponding body parts, so the constrains from the linked body parts may affect the predictions (kinematics and injuries) of the target body region, for example, may influence of neck constrain forces on head [1] and upper body mass on lower limbs [9]. Therefore, reconstruction of real world pedestrian injuries using a full body model is likely to be more valid. The Total Human Model for Safety (THUMS) is an example of a full body pedestrian model widely used in studies of pedestrian injuries [3], [13], [29]. However, evaluation analysis of the THUMS capability for predicting pedestrian injuries in real world collisions is still scarce.

On the other hand, in developing countries with wide rural areas, like China, minivans are far more popular than developed countries with the advantages of large passenger carrying capacity, low price and low fuel consumption. It was reported that over 30,000 minivans were involved in accidents in 2012 in China, which caused 6,865 deaths and around 35,000 injured [12]. Thus, pedestrian safety issue in minivan collisions is worthy of attention in China. But biomechanical analyses of pedestrian injuries in minivan collisions are still rare, especially those based on reconstruction of real world cases.

Therefore, the purpose of this study is to evaluate the capability of the THUMS pedestrian model in predicting pedestrian injuries (including head, thorax and lower limbs injuries) and to investigate pedestrian injury mechanisms in minivan collisions via numerical reconstruction of a real world minivan-to-pedestrian impact case.

2. Materials and methods

2.1. Information of the minivan-to-pedestrian impact case

A minivan-to-pedestrian impact case which has detailed information about vehicle, pedestrian, impact scenario and injuries was selected for this study. This accident case was captured in China by the In-depth Investigation of car Accidents in Changsha (IVAC) work team. The impact scenario is shown in Fig. 1 as the onsite sketching which includes the initial direction of vehicle driving and pedestrian walking, impact and final locations of the vehicle and pedestrian. This is a typical pedestrian accident with the victim being struck by a running minivan from the right side when crossing the road. Basic information of this case is summarized in Table 1, including the details and their sources. The impact speed was calculated in a previous study [12] based on the data from multi-body modeling reconstruction, kinetic energy theorem calculation (v = 3.6*2 μgL$^{1/2}$: v is the impact speed in km/h, μ is the friction coefficient = 0.7 for dry road surface, g = 9.8 m/s^2 and L is the breaking distance)

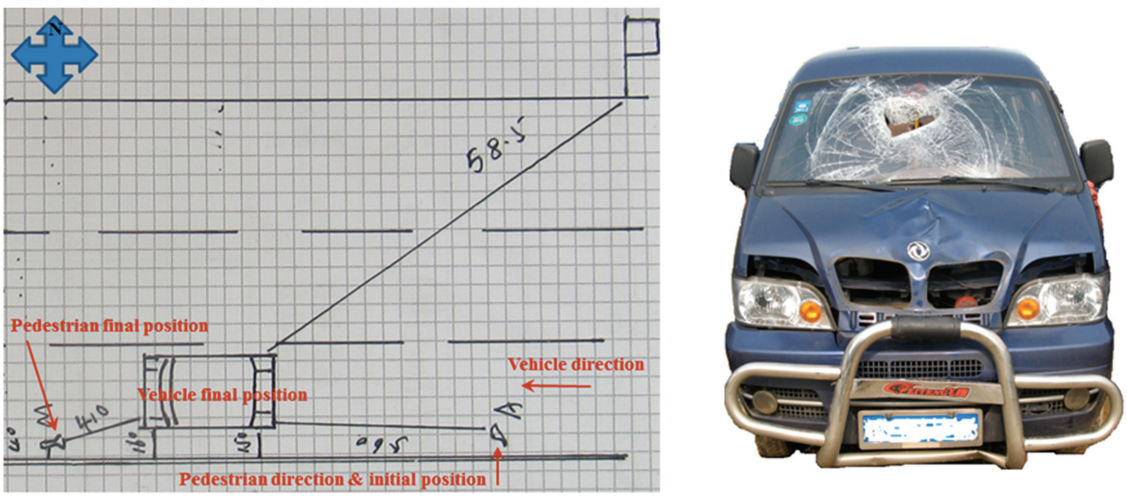

Fig. 1. Field sketching and involved minivan of the accident case

Table 1. Summary of the crash case

Item	Category	Details	Source
Minivan	Model	2008 Dongfeng EQ6362PF	Manufacturer
	Dimension [mm]	3640 × 1560 × 1925	
	Mass [kg]	985	
	Impact speed [km/h]	45	Calculation
Pedestrian	Age [years]	40	Victim
	Height [cm]	172	
	Weight [kg]	68	
Main injuries from primary contact	Lower limb	Right tibia shaft fracture (AIS2)	Hospital
	Thorax	Bilateral pulmonary contusion (AIS4) Multiple rib fractures (AIS3)	
	Head	Concussion (AIS2)	

and an interview with the driver. The injuries of the victim's head, thorax and lower limb were extracted from the injury report provided by the hospital and the corresponding Abbreviated Injury Scale (AIS) level for each injury was given according to the AIS code system [5].

2.2. Human body FE model

The Total Human Model for Safety (THUMS) Academic Version 4.02 AM50 pedestrian fracture model was used and configured into a walking gait stance to simulate the victim involved in the above accident case (Fig. 2). The selection of this gait stance was based on the impact scenario (pedestrian was struck from the right side), deformations of the minivan (Fig. 1) and injury information. In particular, two deformed marks in the bull bar reflect the step distance, the relative position between the bonnet and windscreen deformation center and the observed face bruises from glass fragments reply a forward rotation of the upper body (body rotates forward around the superior-inferior axis of the pedestrian). Thus, a gait stance of struck leg (right) lagging and non-struck leg (left) leading with a certain step distance was selected according to previous studies [3], [13].

The THUMS Academic Version 4.02 AM50 pedestrian fracture model was built based on the CT scan data of a 39-year-old male with a height of 173 cm and a weight of 77.3 kg, which generally match the posture of the victim. This model can predict brain and internal organ injuries, skeletal fractures and ligament ruptures [22]. The biofidelity of the models for segment body region components and the kinematics of the whole body model were validated against cadaver tests [27].

2.3. Minivan front FE model

A minivan front FE model was extracted from a full scale FE model of a production minivan which is close to the design of the vehicle involved in the accident case (Fig. 3). The initial minivan FE model

Fig. 2. THUMS Academic Version 4.02 AM50 pedestrian model and gait stance

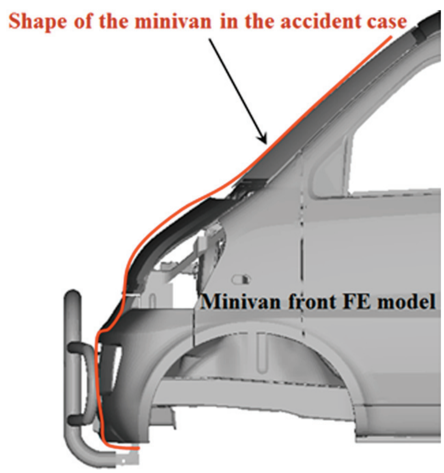

Fig. 3. Comparison of the shape of the minivan front FE model and the minivan involved in the accident case

has been validated against rigid-wall frontal impact test data in our project and used in simulations of vehicle-pedestrian collisions in previous studies [7], [26]. In the current study, the windscreen model was redefined using a valid approach proposed by a previous study based on head impactor-to-windscreen crash test data [19]. Unfortunately, the difference in stiffness between the model and real van is not able to be compared due to lack of data, but this difference is not likely to be very big considering the very similar cost of manufacture for vehicles at this level.

2.4. Simulation setup and injury assessment metrics

A minivan-to-pedestrian impact simulation model was then developed using the above pedestrian and minivan front FE models, where the initial contact location was defined based on the deformation traces on the accident minivan (Fig. 1). The impact speed was defined as 45 km/h from the right side of the pedestrian according to the case information (Fig. 1, Table 1). Similar to previous studies [3], [13], friction coefficients of 0.3 and 0.7 were applied to contacts of minivan-to-pedestrian and the ground-to-pedestrian feet, respectively.

Injury metrics, such as leg lateral bending moment, Thoracic Trauma Index (TTI), Normalized Half Thorax Deflection (NHTD-the maximum change in distance between right side and the sternum-to-spine centerline normalized with respect to the initial full thorax width) as well as the maximum Head Impact Power (HIP_{max}) and Cumulative Strain Damage Measure at the critical level of 0.2 ($CSDM_{0.2}$) were extracted or calculated based on the impact simulation output (the formulations for TTI and HIP are provided in the Appendix A). All selected injury metrics were wildly used for assessing injuries of the corresponding body regions, as observed in the accident case (Table 1), particularly leg lateral bending moment is for tibia fractures [10], TTI and NHTD are for thoracic injuries [11], and HIP_{max} [16] and $CSDM_{0.2}$ [8] are for concussion. The selection of HIP for brain injury prediction was also based on our recent findings where HIP showed a better correlation with real pedestrian brain injuries than other kinematics-based injury criteria such as BrIC, HIC, GAMBIT and RIC [24]. Then, the probability of each injury was calculated based on these predicted injury metrics using the corresponding injury risk curves derived from previous studies and was compared with the injuries observed from the real world case.

3. Results

3.1. Kinematic response

In Figure 4, the whole-body kinematics of the THUMS model during the impact was shown. An obvious upper body forward rotation was predicted and the contact starts from thigh to the upper edge of the bull bar, followed by lower leg-to-the-bull bar frame, pelvis-to-the-bonnet leading edge, thorax-to-the-bonnet rear/widescreen lower frame and head-to-the windscreen. In Figure 5, the deformation traces in the minivan between the simulation and accident data

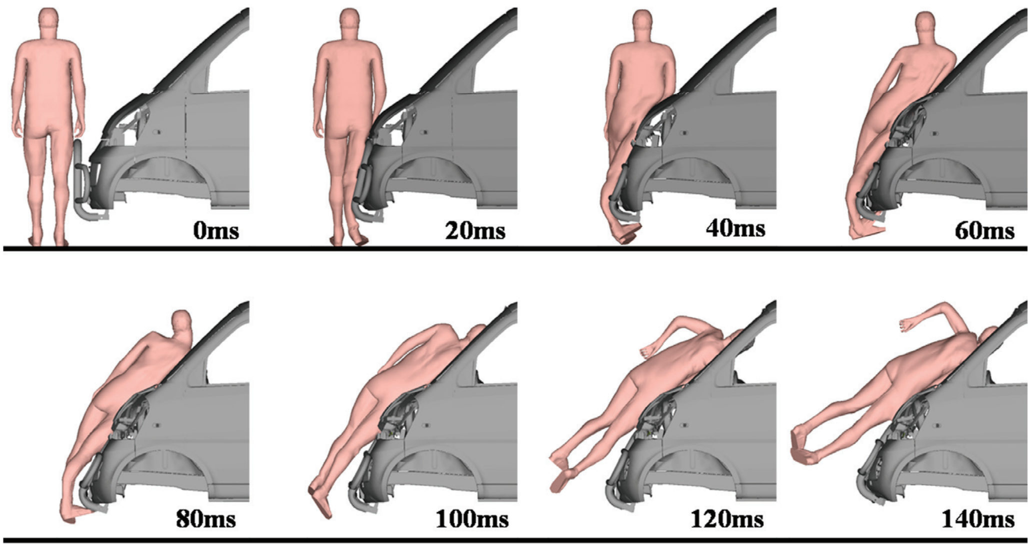

Fig. 4. Predicted kinematics of the THUMS pedestrian model in the collision case

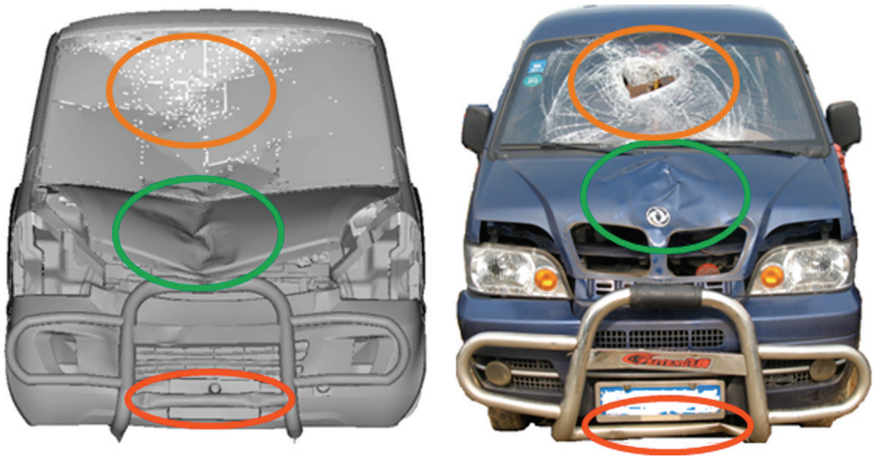

Fig. 5. Comparison of deformation traces in the minivan between the simulation and accident data

were compared. Clearly, the locations and characteristics of the predicted deformation traces in the minivan FE model can generally match that of the real minivan, excepting the run through broken windscreen.

3.2. Injury prediction

In Figure 6a the location of the right tibia fracture between the FE simulation and X-ray data were compared. Based on the figure, it can be clearly stated that the location of the predicted tibia fracture is similar to that of the real case, but not like the real world case, in the simulation the fibula was also fractured and the detailed fracture characteristic of the tibia could not been predicted. In Figure 6b, the predicted pedestrian thorax deflection together with the CT data from the hospital were shown. Significant thorax deflection and six rib fractures in the right side were predicted, which refers to the severe nidus of right lung injury as observed from the chest CT data.

In Figure 7a, the predicted time history of the lateral bending moment for the struck leg and the peak value in the injury risk curves of tibia fracture were shown [10]. At the fracture time (21 ms), leg lateral bending moment reached the maximum value of 205 Nm, which indicates a 13–40% risk of tibia fracture. The predicted TTI and NHTD in the risk curves of thorax injuries proposed by [11] were shown in Fig. 7b. The predicted TTI value of 215 g indicates a 98% risk of AIS3+ and 86% risk of AIS4+ thorax injuries, respectively. Similarly, the predicted NHTD value of 0.34 also shows high risk of AIS3+ (92%) and AIS4+ (73%) thorax injuries. Figure 7c shows the predicted HIP_{max} and $CSDM_{0.2}$ values in the injury risk curves for concussion [8], [16]. The predicted HIP_{max} value of 23 kW and $CSDM_{0.2}$ value of 0.36 indicate a 98% and 26% risk of concussion, respectively.

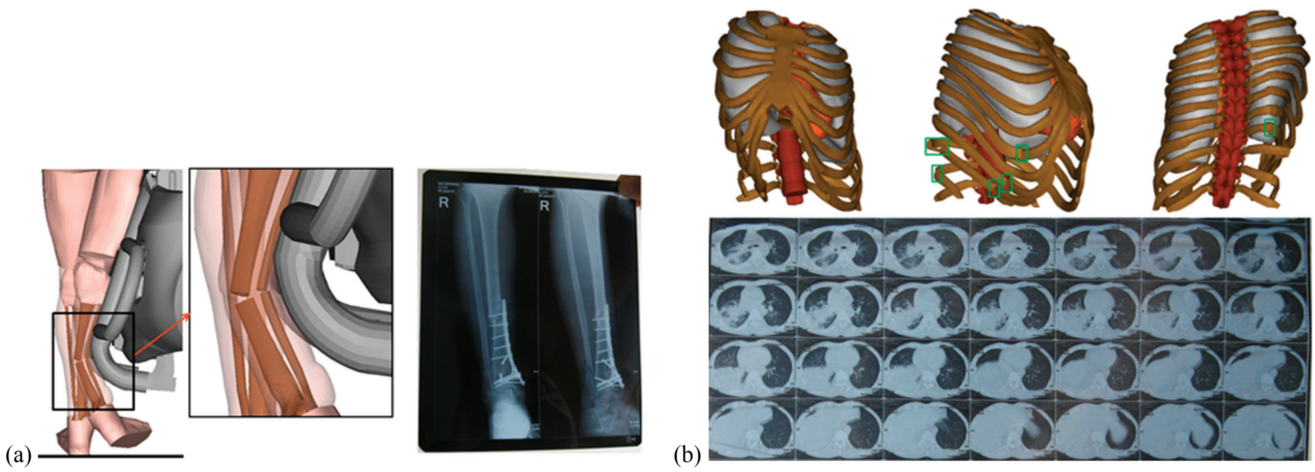

Fig. 6. Predicted long bone fractures (a) and thorax deflection and rib fractures (b) together with X-ray and CT data from the hospital

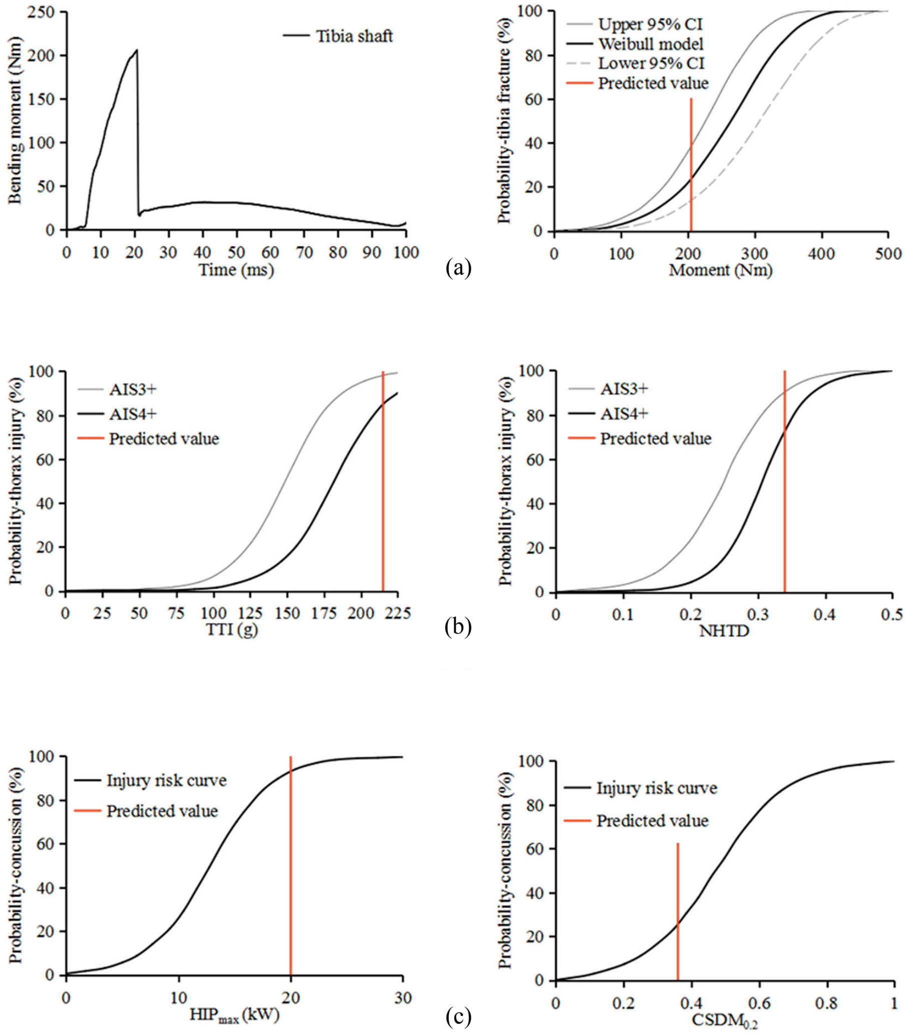

Fig. 7. Predicted leg lateral bending moment time history and the peak value in the tibia fracture risk curves adapted from Kerrigan et al. [18] (a), TTI and NHTD values in the thorax injury risk curves adapted from Kuppa [20] (b), HIP_{max} and $CSDM_{0.2}$ in the risk curves for concussion adapted from Newman et al. [28] and Huang et al. [16] (c)

4. Discussion

4.1. Injury predicting capability

The reconstruction of the impact boundary condition (gait stance, impact direction and pedestrian orientation) of the selected minivan-to-pedestrian collision case was firstly evaluated with the good matches of deformation traces on the minivan front between the predictions and the real world case and the clear upper body forward rotation (Figs. 4 and 5). This provides basic validity for injury prediction analysis.

However, the predicted lower limb injuries are not in line with the real case, where the left fibula which is non-injured in the real case fractured in the simulation (Fig. 6a). In fact, the injury type of tibia fracture only (24%) is not as common as the case with both tibia and fibula being fractured (54%) in real world vehicle-to-pedestrian collisions [18]. The THUMS pedestrian model predicted the most common leg long bone fracture type. However, the predicted tibia fracture risk of 13–40% based on leg lateral bending moment (205 Nm) is quite low (Fig. 7a), compared to the predicted von Mises stress and maximum strain. Figure 8 shows that the predicted maximum tibia von Mises stress prior to the fracture reached 192 MPa, which is substantially higher than the average yield stress of tibial cortical bone (129 MPa) from cadaver tests [21]. The maximum strain exceed the threshold of 2.14% (control parameter of fracture in the model) defined in the THUMS fracture model, which is also significantly higher than the average ultimate strain of tibial cortical bone (1.5%) from cadaver tests [21]. Similarly, low fracture risk of bending moment versus high fracture risk of maximum strain was also predicted for the tibia in a previous study using the recent version (4.01) THUMS pedestrian model [29]. Thus, these results may suggest that the THUMS tibia model is kind of too "soft" in predicting bending moment, compared to stress and strain, which means that further study of the material properties might be needed.

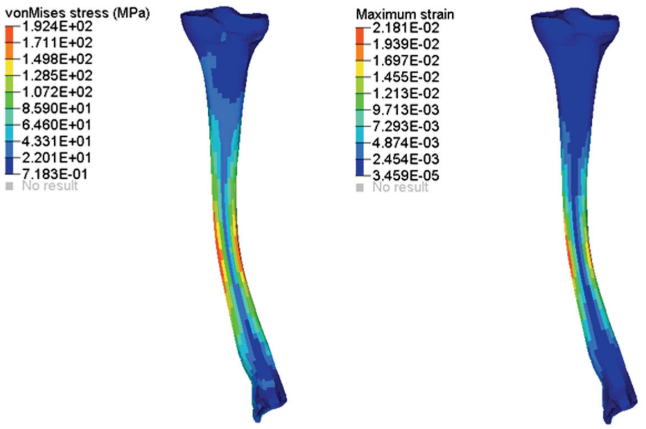

Fig. 8. Predicted right tibia stress and strain distribution prior to the fracture

The results in Fig. 6b and 7b indicate that the predicted thorax injuries are similar to that observed from the real collision case. In particular, the predicted six rib fractures and high AIS3+ (>90%) and AIS4+ (70%) thorax injury risks (referring to TTI and NHTD) show good agreement with the real multiple rib fractures (AIS3) and bilateral pulmonary contusion (AIS4) (Table 1), respectively. These predicted thorax injury risk might be higher if a minivan FE model with similar stiffness to the real case were used, since the windscreen lower frame of the minivan FE model seems to be softer than the real case car considering the larger deformation of this area in the simulation compared to the accident data (Fig. 5). Nevertheless, these findings proved the goodness of the THUMS model in predicting real world thorax injuries. This has also been verified in previous reconstruction studies of a real impact case [6] and cadaver tests [29].

For brain injuries, the predicted injury risk of concussion varies from injury metrics, the concussion risk based on the $CSDM_{0.2}$ (26%) is significantly lower than that based on the HIP_{max} (98%) (Fig. 7c). This may be largely caused by the fact that the $CSDM_{0.2}$ curve and HIP_{max} curve are not from the same sample, as the $CSDM_{0.2}$ curve was based on reconstruction of 43 vehicle-to-pedestrian collisions using a FE human head model [8] and the latter was built from reconstruction of 24 professional football cases using the Hybrid III ATDs (Anthropopathic Test Device) [16]. In addition, the differences in definitions of materials for brain tissues and modeling choice for the brain-skull interface between the THUMS head model and the FE human head model used by Huang et al. [8] may also lead to difference in brain strain prediction [25], and thus affecting the predicted concussion injury risk. Furthermore, the stiffness difference between the minivan FE model and the real case car may have effects on brain strain and HIP prediction due to the influence on shoulder and head contact boundary [3], [20], and then affecting the level of predicted injury risk. Therefore, it is difficult to evaluate the biofidelity of the THUMS head model for brain injury prediction based on the results of the current study. However, these results may suggest to further check the materials of the THUMS brain model in terms of strain prediction, considered together with the comments from previous findings using the THUMS head model, where the stiffness of the THUMS brain model was adjudged somewhat too high [25].

4.2. Injury mechanism in minivan-to-pedestrian collision

Fig. 6a shows that the tibia and fibula fractures occurred just below the beam of the bull bar. This implies that the lateral bending caused by the inertia mass of leg below the beam and the concentrated contact force between pedestrian's leg and the beam are the key mechanisms for the tibia fracture. To verify this observation, a simulation using a FE minivan model without the bull bar (all other conditions are the same as in the reconstruction simulation) was conducted and the predicted leg bending is shown in Fig. 9.

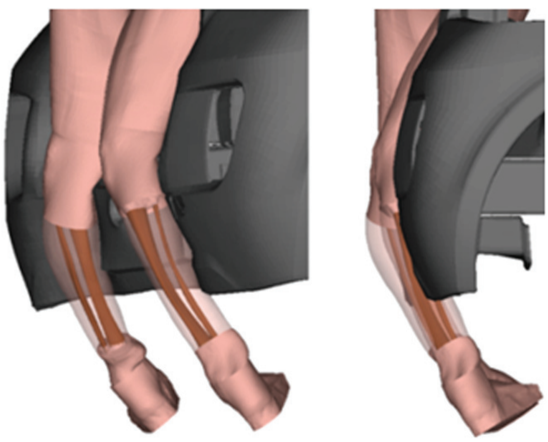

Fig. 9. Pedestrian lower limb dynamic response in the collision with a minivan front without the bull bar

The removal of the bull bar significantly reduced leg bending and no fracture was observed in the comparison simulation. This indicates that bull bars could raise pedestrian lower limb injury risk, and thus it suggests to removing bull bars from the minivan front for pedestrian lower limb protection similar to previous studies [7].

Significant thorax deflection was predicted in the struck side, which was caused by contact with the bonnet end/windscreen lower frame and resulted in six rib fractures and serious compression to the right lung (Figs. 4 and 6b). The inertia force from the heart leaded compression to the left lung. The largest ribcage deflection occurred at the lower thorax level (8th–12th ribs) due to the relatively flat structure of the minivan front and the tapered shape of human ribcage in the coronal plan. This is probably an important reason for the higher thorax injury risk in minivan-to-pedestrian collisions, compared to bonnet type vehicles where more evenly contact between pedestrian thorax and vehicle was observed. Similar understanding of pedestrian thorax injury mechanism in flat end vehicle collisions was also reported in previous studies based on accident data [12] and FE simulations [26]. The above kinematic predictions are in agreement with the CT data well, where the nidus in both right and left lung is at the lower thorax level, and the nidus in the right lung starts from the outside while that in the left lung starts from the internal side (Fig. 6b).

Brain strain is regarded as an effective predictor for diffuse brain injury [20]. Thus, the time history curves for head impact power (HIP) and head linear and angular acceleration were shown together with the brain strain nephogram (at different points of time) to have a better understanding on the mechanism of concussion (Fig. 10). These data indicate that head angular acceleration shows better match with the brain strain than HIP and linear acceleration. This implies that angular acceleration plays a dominant role on concussion, which is similar to the observation in a previous study based on tests using live subhuman primates and physical models [15].

4.3. Limitations

There are several limitations to this study. Only one crash was reconstructed due to the lack of detailed injury data (X-ray and CT) in other cases, reconstructions of more real world cases are needed in the further study to evaluate the injury predicting capability of the THUMS model and to understand pedestrian injury mechanisms in minivan collisions. There could

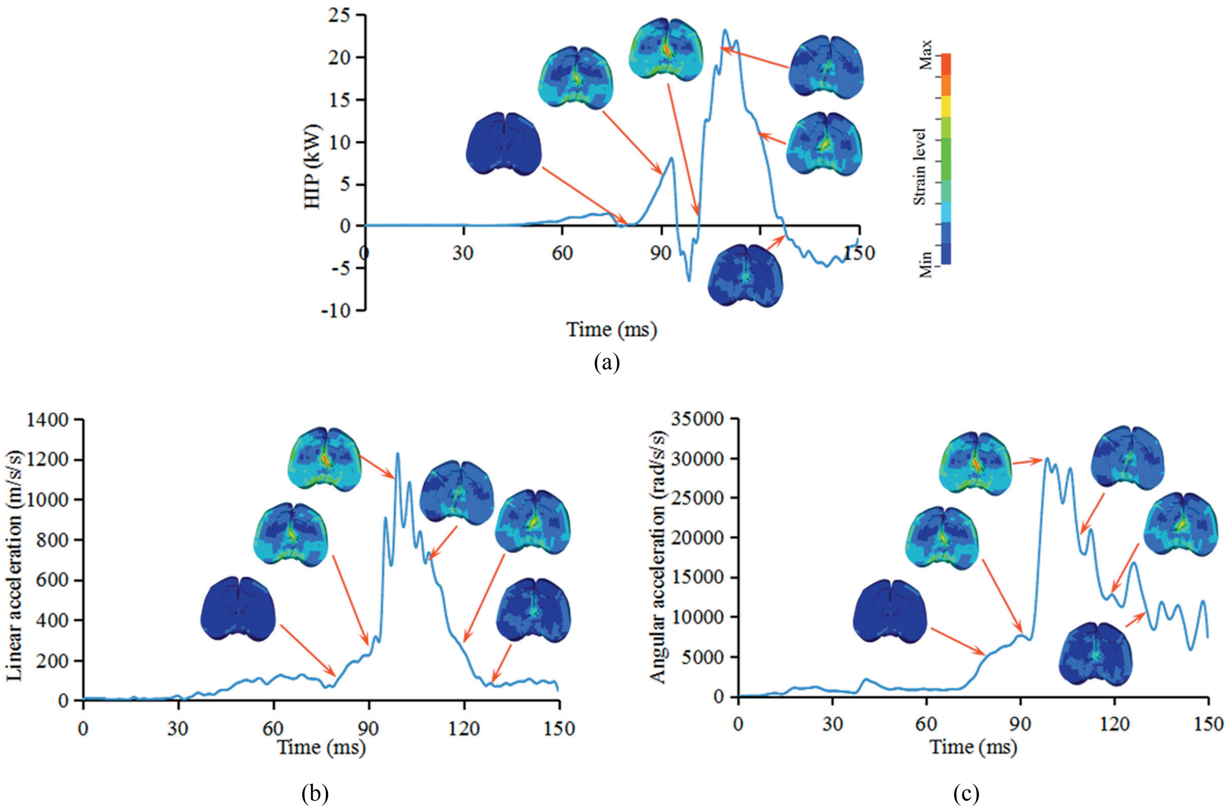

Fig. 10. Predicted time history curves for HIP (a), head linear (b) and angular (c) acceleration and brain strain nephogram

be some differences in stiffness between the minivan FE model and the real case minivan, which could affect injury predicting accuracy. More open access FE models of real world vehicles would be helpful for future studies of crash reconstruction. The THUMS model (77.3 kg) seems to be fatter than the victim (68 kg), which may affect the impact power and contact loading transmission. However, previous study of accident data showed that weight within the range of 61–90 kg has no significant influence on pedestrian risk [30]. Further study is needed to verify this data. The pedestrian posture wax approximately estimated based on logical inference, which could affect pedestrian dynamic responses and injuries [3], [13]. The concussion risk curves applied in this study were derived from reconstruction analysis using either isolate human head FE models [8] or ATDs [16]. Both have limitations in representing full scale human body.

5. Conclusions

A real world minivan-to-pedestrian crash was reconstructed using the THUMS pedestrian model. Comparisons of predictions and accident data indicate that the THUMS has a good capability in predicting pedestrian thorax injuries observed in the real world case, but a lower prediction of leg bending moment and brain strain even when tibia/fibula fractures and high HIP value were predicted. Analysis of injury mechanism in the minivan collision shows that the extra bull bar concentrates crash load to pedestrian's leg and raises tibia/fibula fracture risk; thorax injuries in the struck side are mainly from direct contact and ribcage deflection at the lower chest level; lung injuries in the non-struck side could be caused by inertia force from the heart; rotational acceleration shows good match with brain strain and could be the key mechanism for concussion. Furthermore, the method demonstrated in the current study could be used for more extended research on reconstruction of in-depth accidents and further improvement of human body models.

Acknowledgements

This work was supported by the National Natural Science Foundation of China (Grant Nos. 51805162 and 51605407), Natural Science Foundation of Hunan Province (Grant No. 2018JJ3532), Scientific and Technological Research Program of Chongqing Municipal Education Commission (Grant No. KJQN201801107), Foundation of Zhejiang Province Key Laboratory of Automobile Safety and Educational Commission of Hunan Province of China (Grant No. 17A068). All simulations using the Total Human Model for Safety (THUMS) Academic Version pedestrian model in this research were conducted at Chongqing University of Technology. The authors gratefully thank Dr. Jikuang Yang from Hunan University (China)/Chalmers University of Technology (Sweden) for providing with the IVAC accident data and minivan FE model.

References

[1] Alvarez V., Halldin P., Kleiven S., *The influence of neck muscle tonus and posture on brain tissue strain in pedestrian head impacts*, Stapp. Car Crash J., 2014, 58, 63–101.

[2] Cai Z., Lan F., Chen J., *Development and validation of a human biomechanical model for rib fracture and thorax injuries in blunt impact*, Comput. Method. Biomec., 2015, 18(9), 974–980.

[3] Chen H., Poulard D., Crandall J., Panzer M., *Pedestrian response with different initial positions during impact with a mid-sized sedan*, Proceedings of the 24th International Technical Conference of Enhanced Safety of Vehicles (ESV), 2015, Gothenburg, Sweden; Paper No. 15-0391.

[4] Eppinger R., Morgan R., Marcus J., *Development of dummy and injury index for NHTSA's thoracic side impact protection research program*, SAE Technical Paper No. 840885, 1984.

[5] Gennarelli T., Wodzin E., *AIS 2005: a contemporary injury scale*, Injury, 2006, 37(12), 1083–1091.

[6] Golman A., Danelson K., Miller L., Stitzel J., *Injury prediction in a side impact crash using human body model simulation*, Accid. Anal. Prev., 2014, 64, 1–8.

[7] Guo W., Yang J., *Effects of bull bars on head and lower extremity injuries in vehicle-pedestrian collision*, Proceedings of the 3rd International Conference on Digital Manufacturing and Automation (ICDMA2012), 2012, Guilin, China.

[8] Huang J., Peng Y., Yang J., Otte D., Wang B., *A study on correlation of pedestrian head injuries with physical parameters using in-depth traffic accident data and mathematical models*, Accid. Anal. Prev., 2018, 119, 91–103.

[9] Isshiki T., Konosu A., Takahashi Y., *Development and evaluation of the advanced pedestrian legform impactor prototype which can be applicable to all types of vehicles regardless of bumper height-Part 1: finite element model*, Proceedings of the International Research Council on Biomechanics of Injury (IRCOBI) Conference, 2016, Malaga, Spain.

[10] Kerrigan J., Drinkwater D., Kam C., Murphy D., Ivarsson B., Crandall J., Patrie J., *Tolerance of the human leg and thigh in dynamic latero-medial bending*, Int. J. Crashworthiness, 2004, 9 (6), 607–623.

[11] Kuppa S., Eppinger R., Mckoy F., Nguyen T., Pintar F., Yoganandan N., *Development of side impact thoracic injury criteria and their application to the modified ES-2 dummy with rib extensions (ES-2re)*, Stapp. Car Crash J., 2003, 47, 189–210.

[12] Li G., Nie J., Yang J., *A study on injuries and kinematics in pedestrian accidents involved minivan and sedan*, Reports on the 5th International Conference on ESAR (Expert Symposium Accident Research), 2012, Hannover, Germany.

[13] Li G., Yang J., Simms C., *The influence of gait stance on pedestrian lower limb injury risk*, Accid. Anal. Prev., 2015, 85, 83–92.

[14] Li G., Wang F., Otte D., Cai Z., Simms C., *Have pedestrian subsystem tests improved passenger car front shape*, Accid. Anal. Prev., 2018, 115, 143–150.

[15] MARGULIES S., THIBAULT L., *A proposed tolerance criteria for diffuse axonal injury in man*, J. Biomech., 1992, 25 (8), 917–923.
[16] NEWMAN J., SHEWCHENKO N., WELBOURNE E., *A proposed new biomechanical head injury assessment function – the maximum power index*, Stapp. Car Crash J., 2000, 44, 215–247.
[17] NIE J., LI G., YANG J., *A study of fatality risk and head dynamic response of cyclist and pedestrian based on passenger car accident data analysis and simulations*, Traffic Inj. Prev., 2015, 16(1), 76–83.
[18] OTTE D., HAASPER C., *Characteristics on fractures of tibia and fibula in car impacts to pedestrians and bicyclists-influences of car bumper height and shape*, Ann. Proc. Assoc. Adv. Automot. Med., 2007, 51, 63–79.
[19] PENG Y., YANG J., DECK C., WILLINGER R., *Finite element modeling of crash test behavior for windshield laminated glass*, Int. J. Impact Eng., 2013, *57*(7), 27–35.
[20] SIMMS C., WOOD D., *Pedestrian and Cyclist Impact – A Biomechanical Perspective*, Springer, 2009.
[21] TAKAHASHI Y., KIKUCHI Y., KONOSU A., ISHIKAWA H., *Development and validation of the finite element model for the human lower limb of pedestrians*, SAE Technical Paper No. 2000-01-SC22.
[22] Toyota Motor Corporation, Documentation: Total Human Model for Safety (THUMS) AM50 pedestrian/occupant model academic version 4.02_20150527, 2015.
[23] WANG B., YANG J., OTTE D., PENG Y., *A study of long bone fractures via reconstruction of pedestrian accident using multi-body system and lower extremity FE model*, J. Mech. Med. Biol., 2015, 15(1), 1550016.
[24] WANG F., CAI J., WANG B., HAN Y., LI G., LI F., *Investigation of prediction effectiveness of brain injury criteria on injury risk through reconstruction of pedestrian impact accidents*, China Journal of Highway and Transport, 2018, 31 (4), 231–240, (in Chinese), available at: http://zgglxb.chd.edu.cn/CN/Y2018/V31/I4/231.
[25] WANG F., HAN Y., WANG B., PENG Q., HUANG X., MILLER K., WITTEK A., *Prediction of brain deformations and risk of traumatic brain injury due to closed-head impact: quantitative analysis of the effects of boundary conditions and brain tissue constitutive model*, Biomech. Model. Mechan., 2018, 17, 1165–1185.
[26] WANG F., YU C., LI G., HAN Y., WANG B., YANG J., LAN D., *A study on influence of minivan front-end design and impact velocity on pedestrian thorax kinematics and injury risk*, Appl. Bionics. Biomech., 2018, 7350159, 1–8.
[27] WATANABE R., MIYAZAKI H., KITAGAWA Y., YASUKI T., *Research of collision speed dependency of pedestrian head and chest injuries using human FE model (THUMS version 4)*, Proceedings of the 22nd International Technical Conference on the Enhanced Safety of Vehicles Conference (ESV), 2011, Washington, DC, Paper No. 11-0043.
[28] World Health Organization, Global Status Report on Road Safety2015, Geneva, Switzerland, 2015.
[29] WU T., KIM T., BOLLAPRAGADA V., POULARD D., CHEN H., PANZER M., FORMAN J., CRANDALL J., PIPKORN B., *Evaluation of biofidelity of THUMS pedestrian model under a whole-body impact conditions with a generic sedan buck*, Traffic Inj. Prev., 2017, 18(S1), S148–S154.
[30] ZHANG G., CAO L., HU J., YANG K., *A field data analysis of risk factors affecting the injury risks in vehicle-to-pedestrian crashes*, Ann. Proc. Assoc. Adv. Automot. Med., 2008, 52, 199–214.

Appendix A: Definition for TTI and HIP

The TTI is an acceleration criterion which takes account of the age and weight of the test subject as well as the spinal acceleration [4]. The TTI is defined as follows:

$$\mathrm{TTI} = 1.4 * \mathrm{age} + \frac{1}{2}(\mathrm{RIB}_{\mathrm{acc}} + \mathrm{T12}_{\mathrm{acc}})\frac{M}{M_{\mathrm{ref}}}, \quad \text{(A1)}$$

where age is given in years, $\mathrm{RIB}_{\mathrm{acc}}$ [g] is the maximum lateral acceleration of the fourth or eighth ribs (depending on which is higher) on the ipsilateral side, $\mathrm{T12}_{\mathrm{acc}}$ is the maximum lateral acceleration [g] of the twelfth thoracic spine, M [kg] is the subject's mass and M_{ref} [kg] is the reference mass (75 kg as a 50th% adult male).

Newman et al. [16] proposed the Head Impact Power (HIP) index, which takes all head motions in six degrees into consideration for assessing brain injury. The HIP can be described as follows:

$$\begin{aligned}\mathrm{HIP} &= ma_x \int a_x dt + ma_y \int a_y dt + ma_z \int a_z dt \\ &+ I_{xx}\alpha_x \int \alpha_x dt + I_{yy}\alpha_y \int \alpha_y dt + I_{zz}\alpha_z \int \alpha_z dt,\end{aligned} \quad \text{(A2)}$$

where m and I are the mass and moments of inertia for the human head respectively, while a and α are the linear and rotational accelerations of the head respectively. The subscripts show the acceleration and inertial components and the maximum HIP was proposed for predicting brain injuries (especially for concussion).